Not Duplicate

CONF-8506178--2

LA-UR--85-2281

DE85 014069

TITLE: RELATIVISTIC HYDRODYNAMICS, HEAVY ION REACTIONS AND ANTIPROTON ANNIHILATION

AUTHOR(S): D. Strottman

SUBMITTED TO. Proceedings of the Cretan International Meeting on Subatomic Physics, Heraklion, Greece, June 1985

DISCLAIMER

Los Alamos Los Alamos National Laboratory
Los Alamos, New Mexico 87545

RELATIVISTIC HYDRODYNAMICS, HEAVY ION REACTIONS AND ANTIPROTON ANNIHILATION

D. Strottman
Theoretical Division, Los Alamos National Laboratory
Los Alamos, New Mexico 87545

ABSTRACT

The application of relativistic hydrodynamics to relativistic heavy ions and antiproton annihilation is summarized. Conditions for validity of hydrodynamics are presented. Theoretical results for inclusive particle spectra, pion production and flow analysis are given for medium energy heavy ions. The two-fluid model is introduced and results presented for reactions from 800 MeV per nucleon to 15 GeV on 15 GeV per nucleon. Temperatures and densities attained in antiproton annihilation are given. Finally, signals which might indicate the presence of a quark-gluon plasma are briefly surveyed.

Invited talk at the Cretan International Meeting on Subatomic Physics, Heraklion, Greece, June 1985

One of the new and exciting areas of nuclear physics research today is the study of extreme states of nuclear matter The common tool for the exploration is relativistic heavy ions Lower energy and lighter mass projectiles have been used for years to study aspects of conventional nuclear physics: high-spin states, giant resonances, nuclei off the line of stability, particle-transfer reactions, etc. The common theme heretofore in all these studies was that the nuclear excitation energy was relatively low and the nuclear density ρ was essentially equal to ρ_0, the normal nuclear density

The new accelerators will allow one for the first time to systematically explore much different regimes of nuclear matter. densities several times ρ_0 and internal energies characterized by temperatures exceeding the pion mass. At sufficiently high densities or temperatures a new phase of matter is predicted to occur, namely the quark-gluon plasma, in which the nucleons and mesons lose their individual identity and the quarks are asymptotically free[1,2].

The obvious method to create regimes of high temperature and density is through colliding ultra-relativistic nuclei. A second method proposed to study the quark-gluon plasma, or at least conditions leading to a plasma, is anti-matter annihilation in nuclei[3,4] The study of both processes has only begun, the theoretical tools for both are currently very similar.

The two usual theoretical models are hydrodynamics and the intranuclear cascade model based on the Monte Carlo technique. The two schemes start from very different assumptions In hydrodynamics one assumes a very short mean free path and that a macroscopic continuum approach is valid. The cascade model assumes the nuclei are dilute systems with the binary collisions of the hadrons treated in a classical picture. Each model has advantages and each model has its own vociferous adherants; each also has disadvantages. In this paper we shall deal almost exclusively with versions of the hydrodynamic model

In the next section the equations of non-relativistic hydrodynamics will be discussed; some of the assumptions and range of validity will be presented. Complications of dissipation and turbulence will also be given. In section three the equations will be extended to the relativistic regime; some results from the Bevalac will be given. In section four a two-fluid model will be introduced and applied to reactions of much higher energy Anti-proton annihilation is discussed in section 5. Finally, in section six possible signatures of a quark-gluon plasma will be summarized.

There are several reviews which discuss heavy ions in greater detail[5,6,7,8,9] These reviews in general also discuss models other than fluid dynamics which have been applied to lower energy heavy ion reactions.

2. FLUID DYNAMICS

We begin by recalling the Navier-Stokes equations which describe a non-relativistic fluid with viscosity[10]:

$$\frac{\partial \rho}{\partial t} + \nabla (\vec{v}\rho) = 0 \tag{1}$$

$$\rho[\frac{\partial \vec{v}}{\partial t} + (\vec{v}\cdot\nabla)\vec{v}] = - \nabla P + \eta\Delta\vec{v} + (\zeta + \frac{1}{3}\eta)\nabla\cdot(\nabla\vec{v}) \tag{2}$$

$$\frac{\partial E}{\partial t} + \nabla(\vec{v}E) = \nabla\cdot[-\vec{v}P + (\zeta - \frac{2}{3}\eta)\vec{v}\cdot(\nabla\cdot\vec{v}) + \frac{1}{2}\eta(\vec{v}\cdot\vec{v}) + \eta(\vec{v}\cdot\nabla)\vec{v}]. \tag{3}$$

In these equations ρ is the density of the fluid, $\vec{v}$ the velocity, P the pressure and E is the energy. The coefficients ζ and η are coefficients of viscosity and are here assumed to be independent of position and temperature although they need not be.

There are several mathematical difficulties with these equations, apart from the serious physical worry that they may not adequately describe colliding nuclei. These difficulties are 1) non-linearity, 2) the equations are coupled, and 3) they do not fall into any of the familiar categories of differential equations such as parabolic, hyperbolic or elliptical and hence the solutions will not be readily obtainable. They are also incomplete in that for a three-dimensional problem, eqns. (1) - (3) summarize five equations in six unknowns: ρ, $\vec{v}$, E, and P. However, this is not surprising; the Navier-Stokes equations as written apply to any fluid. The specific properties of the fluid enter through an equation of state

$$P = P\ (E,\ \rho)$$

which summarizes the internal particle-particle dynamics. The equation of state also provides the necessary sixth equation.

The study of the Navier-Stokes equations for situations of interest to nuclear physics has only begun.[11,12] Very little is known about the magnitudes of the coefficients ζ and η. It is also not clear whether the Navier-Stokes equations are the correct equations. Very specific assumptions[13] are made concerning the nature of the particle-particle interaction in the derivation of eq. (2). Fluids which obey eq. (2) are called Newtonian fluids. However, the majority of fluids appear to be non-Newtonian[14] and equations other than (2) are then necessary to describe the flow.

It should also be noted that the solution of the Navier-Stokes

equations may give rise to instabilities. The instabilities are of two types: numerical, which are both annoying and uninteresting, and physical unstabilities. An example of the latter is turbulence; it is known that for certain values of the viscosity coefficient solutions exhibit rapid fluctuations, a characteristic of turbulence. The problem of turbulence is not yet solved with most of the effort restricted to incompressible fluids. Needless to say, nothing has been done in investigating the effects of turbulence in heavy ion reactions.

It may be a moot point to worry which version of the hydrodynamic equations is the more relevant if the conditions during a heavy ion collisions are such that hydrodynamics is never valid. We shall now show that although one can convince oneself that it is not foolish to apply hydrodynamics to heavy ion collisions, neither is it obvious that hydrodynamics is valid.

The conditions for validity of a hydrodynamic approach are: 1) the number of degrees of freedom must be large; 2) a short mean free path; and 3) a sufficient reaction time for thermal and chemical equilibrium to be attained or nearly attained. For a continuum description to be valid, the system should not be too granular; for uranium on uranium the number of hadrons participating - including the produced pions - approaches 10^3. Hence, the number of degrees of freedom is large compared to one, but small compared to that in a true fluid.

The mean free path of a nucleon in nuclear matter may be estimated from $\frac{1}{\rho\sigma}$ where σ is the nucleon-nuclear cross section. At a bombarding energy of 200 MeV σ is around 200 mb (this is an average of the np and pp cross sections[15]) and λ = 0.3 fm. This is λ_{coll}, the mean distance between collisions; the mean stopping distance λ_{stop} is approximately λ_{coll} $(\frac{T}{\Delta T})$ where T is the kinetic energy and ΔT the average loss of kinetic energy per collision. For an incident energy of 200 MeV ΔT is around 125 MeV Hence, a 200 MeV nucleon will penetrate a fm or so into a nucleus, a distance small compared to the nuclear radius. Of course, these values are for central collisions. If the nucleon strikes near the surface, it will penetrate further or even punch through. However, during the reaction ρ will increase and λ_{stop} will decrease.

At higher bombarding energies λ_{stop} will increase for two reasons. First, σ_{NN} decreases to around 40 mb. Second, $\frac{T}{\Delta T}$ also increases; it takes more collisions to stop a nucleon. Hence, λ_{stop} will increase and may even exceed the nuclear radius. At these energies one-fluid hydrodynamics will cease to be valid and the effects of transparency will need to be included.

There remains the question of the domain of applicability of non-relativistic hydrodynamics. There is no obvious boundary beyond which the non-relativistic theory is not valid. Other physical effects such as nuclear transparency also enter. A common standard by which one chooses whether the relativistic version of a theory is necessary is the velocity; for values of $\beta = v/c$ approaching one clearly relativistic effects are important. The non-relativistic expression for the

kinetic energy of a particle with $\beta = 1$ gives 470 MeV and it might be argued this sets an upper limit. However, by use of the correct kinematics, the range of the non-relativistic theory can be extended somewhat. For $\beta = 0.875$ the kinetic energy of an incident projectile is 1 GeV per nucleon in the laboratory frame or 223 MeV in the center-of-velocity frame. This is above the threshold for pion production. It may be reasonably assumed that at 1 GeV per nucleon relativistic effects are already important although some of the gross details may still be predicted by the non-relativistic theory.

3. RELATIVISTIC HYDRODYNAMICS

In this section the modifications necessary to make the Navier-Stokes equation into relativistic equations will be discussed. Before doing so, however, one can anticipate one of the complications in a covariant version of eq. (2). The non-relativistic momentum equation with viscosity is first-order in time but second-order in the spatial variables. Because of the intimate connection between time and space the relativistic version will necessarily be second-order in both the temporal and spatial variables. Consequently, the equations will be more difficult to solve; in particular, the computer storage required will be twice that of the non-relativistic version and will exceed the capabilities of the computers currently being used. We shall therefore disregard dissipative mechanisms in the one-fluid relativistic hydrodynamic models. Some of their effects will be recovered in the two-fluid model discussed in section 4.

A derivation of the relativistic equations including viscosity may be found in references 10 and 16. We shall here present the final results. We first introduce new notation

N = nucleon number density in an arbitrary frame (usually the lab frame)

n = rest frame nucleon number density

ε = rest-frame energy density

$\vec{M}$ = momentum density in an arbitrary frame

E = energy density in an arbitrary frame.

Obviously,

$$N = \gamma n \tag{5}$$

where $\gamma = \frac{1}{\sqrt{1 - \beta^2}}$ and v = velocity of the reference frame with respect to the rest frame and $\beta = v/c$.

$$\text{Then } \frac{\partial N}{\partial t} + \nabla(\vec{v}N) = 0 \quad . \tag{6}$$

One may obtain this from the equation

$$\frac{\partial(nu^{\mu})}{\partial x^{\mu}} = 0 \tag{7}$$

where the four-velocity is defined such that in the rest frame it takes the value $u^{\mu} = (0\ 0\ 0\ 1)$. To obtain the other two equations, recall that energy and momentum are contained in a single second-rank tensor. In the rest-frame of the fluid the tensor takes the form

$$T_{\mu\nu} = \begin{pmatrix} P & 0 & 0 & 0 \\ 0 & P & 0 & 0 \\ 0 & 0 & P & 0 \\ 0 & 0 & 0 & \varepsilon \end{pmatrix}$$

In an arbitrary reference frame one may show that

$$T_{\mu\nu} = (\varepsilon + P)\, u_{\mu}\, u_{\nu} + g_{\mu\nu} P \quad . \tag{8}$$

The equations of motion are

$$\frac{\partial T_{\mu\nu}}{\partial x_{\mu}} = 0 \tag{9}$$

To obtain the equations in less elegant, but more useful form, first take eq. (9) for the spatial components $\mu = 1, 2, 3$.

$$\frac{\partial T_{i\nu}}{\partial x_{\nu}} = \frac{\partial[(\varepsilon+P)u_i u_k + \delta_{ik} P]}{\partial x_k} + \frac{\partial[(\varepsilon+P)u_i u_0]}{\partial x_0}$$

$$= \frac{\partial[\gamma^2(\varepsilon+P)v_i v_k]}{\partial x_k} + \frac{\partial P}{\partial x_i} + \frac{\partial(\gamma^2(\varepsilon+P)v_i)}{\partial t} = 0 \quad ,$$

where we have used $u_{\mu} \equiv (\gamma v_i, \gamma)$.

If we now make the identification

$$M_i = \gamma^2\, (\varepsilon + P)\, v_i \tag{10}$$

for the momentum, the equation becomes

$$\frac{\partial M_i}{\partial t} + \frac{\partial(M_k v_i)}{\partial x_k} = - \frac{\partial P}{\partial x_i} \quad \text{or}$$

$$\frac{\partial \vec{M}}{\partial t} + \nabla(\vec{M}\vec{v}) = - \nabla P \quad . \tag{11}$$

Thus, this relativistic Euler equation has again the exact same form as does the non-relativistic equation without viscosity, with, however, the important proviso that the momentum explicitly contains contributions from the pressure.

The remaining component of eq. (9) is

$$\frac{\partial T_{o\nu}}{\partial x_\nu} = \frac{\partial[(\varepsilon+P)\gamma^2 v_k]}{\partial x_k} + \frac{\partial[(\varepsilon+P)\gamma^2 - P]}{\partial t} \; ;$$

identifying

$$E = \gamma^2(\varepsilon + P) - P \quad , \tag{12}$$

this becomes

$$\frac{\partial E}{\partial t} + \nabla(E\vec{v}) = - \nabla(\vec{v}P) \tag{13}$$

which also looks like the non-relativistic form.

Both the relativistic as well as the non-relativistic Euler equations are scale invariant, i.e., there is no fundamental length defined. This is a direct result of the Euler equation being linear. Thus, any theoretical results obtained for colliding heavy ions are equally valid for colliding neutron stars provided their equation of state is the same. Similarly, the results will depend only on the ratio of the masses of the colliding nuclei. Dissipation obviously does violate scale invariance; this is reflected by the Navier-Stokes equations having second-order as well as first-order terms. An exhaustive discussion of the possible testing of scale invariance by experiments is given in ref. 17.

The pressure, P, which appears in the Euler equations is calculated by means of the equation of state $E(n,T)$, which specifies the total internal energy as a function of n and T. From thermodynamics one has the relation

$$dE = Tds - PdV$$

or

$$P = -\left.\frac{\partial E}{\partial V}\right)_S = n^2 \left.\frac{\partial E}{\partial n}\right)_S \qquad (14)$$

where S is the entropy.

It is usual to divide E into a part arising only from compression and a part which contains all other dependencies

$$E = E_0(n) + I(n, T, \ldots) \quad . \qquad (15)$$

In eq. (15) E_0 is the compressional energy and I the thermal or internal energy.

Compressional energy = $E_0(n) - E_0(n_0)$

Thermal energy = $I = E(n) - E_0(n)$.

The equation of state has been the object of considerable theoretical work and is one of the motivations for studying heavy ion reactions since this is one of the few ways one has the opportunity to systematically study compressed nuclear matter. Antiproton annihilation is a second possible mechanism[4].

Our knowledge of E_0 is scant:

$$E_0(n_0) = -15.96 \text{ MeV}^{18)} \quad ; \qquad (16)$$

$$\left.\frac{\partial E_0}{\partial n}\right)_{n = n_0} = 0 \quad ; \qquad (17)$$

$$K = 9\, n_0^2 \left.\frac{\partial^2 E_0}{\partial n^2}\right)_{n = n_0} \cong 210 \text{ MeV} \pm 30 \text{ MeV}^{19)} \quad . \qquad (18)$$

These equations allow us a very considerable freedom in choosing a form for E_0, and many forms have been used. Some are shown in fig. 1.

Little is known about the dependence of I on density and temperature and it is usual to rely on models to calculate the thermal pressure. Using eqs. (14) and (15)

$$P = n^2 \frac{\partial E_0}{\partial n} + n^2 \left.\frac{\partial I}{\partial n}\right)_S \qquad (19)$$

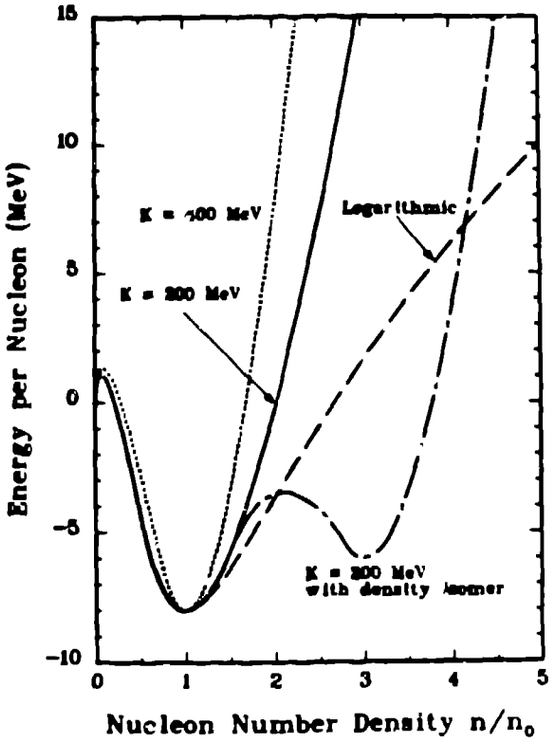

Fig. 1. Four phenomenological forms for the equation of state $\mathcal{E}_0$. The logarithmic form is a logarithmic function of n/n_0 for $n > n_0$, has K = 200 MeV and is identical to the solid curve for $n < n_0$. The other three forms are quadratic functions of $\sqrt{n}$ and become linear in n for large n.

The first term is easily obtained once a form for E_0 is given. For the second term one uses the result from the non-relativistic Fermi gas:

$$n^2 \frac{\partial I}{\partial n}\Big)_S = 2/3\ n\ I \quad ; \tag{20}$$

a relativistic gas:

$$n^2 \frac{\partial I}{\partial n}\Big)_S = 1/3\ n\ I \quad , \tag{21}$$

or some other model. In general we shall assume

$$P = n^2 \frac{\partial E_0}{\partial n} + bn\, I \qquad (22)$$

$$= \chi(n) + bn\, E$$

One may obtain analytic expressions for the maximum compression achievable in a shock for a given incident bombarding energy. The so-called Rankine-Hugoniot relations are derived by assuming a plane shock wave moving with velocity v_s and integrating over the infinitesimal volume which includes the shock front[21,22]. After some algebraic manipulation, one obtains the equation

$$\chi(n)\, n_0(n - n_0\gamma) - E_0 n\, [n_0\, (b\gamma^2 + \gamma^2 - 1) - b\gamma n] = 0$$

which must be solved for n to obtain n_{max}.

In the limit that the energy per nucleon is a constant, $E_0 = n_0 m_0$, $\chi(n) = b\, n\, m_0$ one obtains

$$\left(\frac{n}{n_0}\right)_{max} = \frac{\gamma^2(b+1) - b\gamma - 1}{b(\gamma - 1)} \qquad (23)$$

In the non-relativistic limit

$$\left(\frac{n}{n_0}\right)_{max} = \frac{b+2}{b} \qquad (24)$$

while in the relativistic limit

$$\left(\frac{n}{n_0}\right)_{max} = \frac{b+1}{b}\ \gamma \qquad (25)$$

For a non-relativistic gas b = 2/3 and thus the maximum compression in a non-relativistic theory is 4. Relativistically, the maximum density, eq. (25), increases without limit. For smaller b there is less thermal pressure to resist compression and the maximum compression is larger. Numerical results using two of the zero temperature equations of state, fig. 1, are shown in fig. 2.

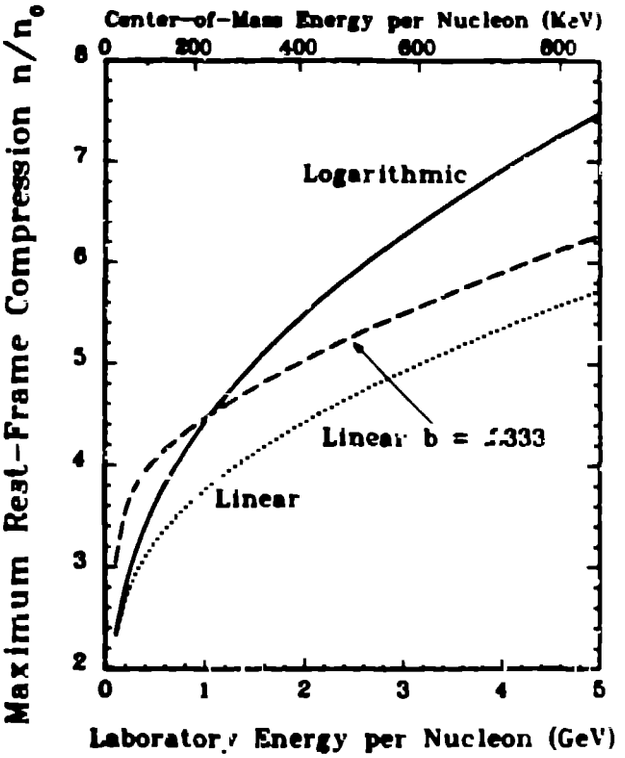

Fig. 2. The maximum compression for two of the equations of state shown in fig. 2. All three curves were calculated with K = 200 MeV. Two curves assumed a thermal energy of a non-relativistic Fermi gas (b = 2/3); the third assumed a relativistic Fermi gas (b = 1/3).

The compressions predicted by the Rankine-Hugoniot relations are somewhat optimistic. Several effects such as nuclear transparency and viscosity will generally tend to decrease the compression reached. (However, the effect of transparency is subtle; less thermal energy may be generated which implies the thermal pressure will be less allowing greater compression.)

The relativistic Euler equations are solved numerically by a finite-difference method known as the particle-in-cell (PIC) method.[23,24] The nuclei are represented by a large number of marker particles which move through a rectangular mesh of fixed, Eulerian cells. Their motion through the cells is governed by finite difference equations obtained from the Euler equations. The PIC method allows a calculation with severely distorted surfaces including those which contain holes or gaps.

In fig. 3 is shown an example of solutions to the equations. The calculation is of two equal mass nuclei colliding at a laboratory energy of 800 MeV per nucleon[29]. The equations are solved in the center-of-mass for which the equivalent energy is 182 MeV per nucleon. Three different impact parameters are shown. For the large impact parameter most of the nucleon matter does not participate in the collision directly. However, a transverse shock wave may be seen in the last two frames.

The b = 0 collision is most dramatic. There is no interpenetra-

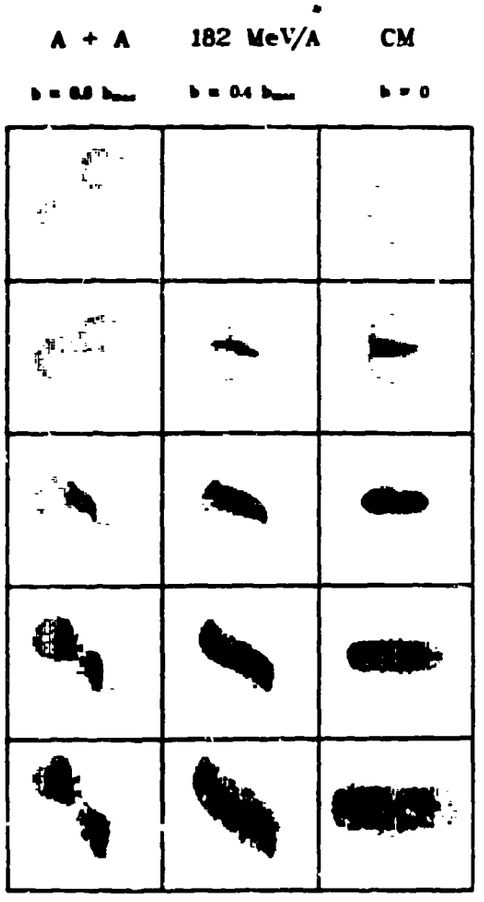

Fig. 3. The time development, in equal time steps, of the projected baryon density in the center-of-mass frame for the three different impact parameters obtained using a three-dimensional relativistic hydrodynamic model. The equivalent laboratory beam energy is 800 MeV per nucleon.

tion of the nuclear matter. The matter at the interface comes to rest and is highly compressed. The 182 MeV incident energy is converted to either compressional or thermal energy which gives rise to a large pressure. The pressure acts isotropically which results in a rapid expansion to the transverse direction or sideways flow. Expansion in the backward direction is originally hindered by the remaining incoming matter.

A comparison between results obtained from hydrodynamic calculations[20] and experiment for 393 MeV per nucleon ^{40}Ne on ^{238}U is given in figure 4. There is quite reasonable agreement between the calculations and experiments and suggests it is not absurd to use hydrodynamics. However, other models such as the intranuclear cascade model obtain similar agreement. Thus although the comparison is encourging, the data does not rule out other models.

A difficulty with inclusive data such as that shown in figure 4 is that it includes contributions from all impact parameters. It was suggested that by triggering on events of high multiplicity, one would bias the selection of events to small impact parameters. The resulting data[26] suggests the presence of sideward flow in agreement with hydrodynamics[27] and reinforces the suggestion that fluid dynamics is able to predict the gross details of heavy ion reactions.

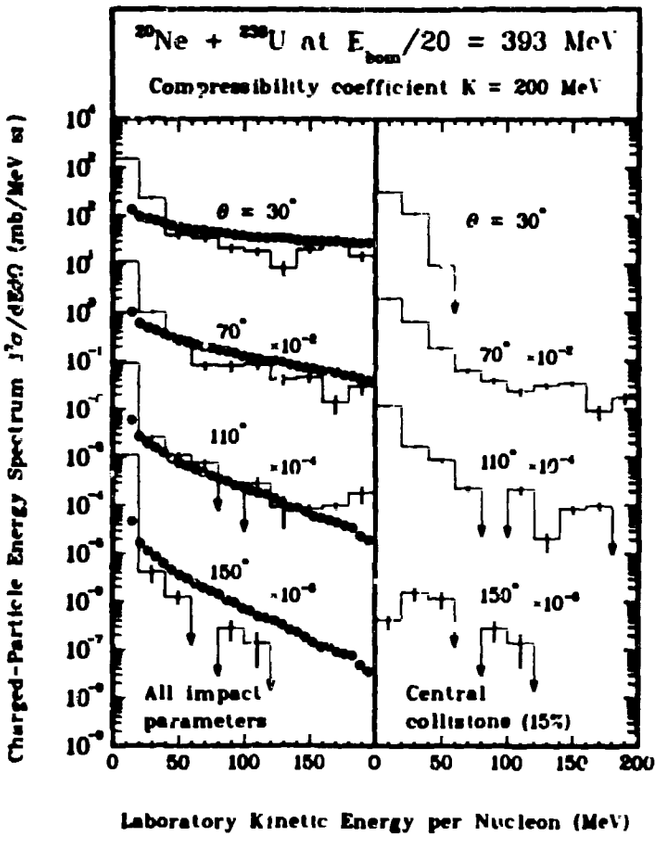

Fig. 4. Charged-particle energy spectrum $d^2\sigma/dEd\Omega$ calculated with an equation of state having K = 200 MeV. The experimental data is from reference 25. The vertical lines on the calculated curve indicate statistical errors.

The result alluded to above that different models with widely divergent initial assumptions give essentially the same differential cross section when only one particle was detected suggests that much of the crucial information is averaged or filtered out. A more demanding test would be to detect all particles, or at least all charged particles, resulting from a reaction. So-called 4π detectors capable of detecting all charged particles have been constructed at the Bevelac.

Several methods of global analysis have been suggested[28,29,30]. The first model[28] constructs a kinetic energy flow tensor

$$F_{ij} = \Sigma \frac{p_i(\lambda)p_j(\lambda)}{2m_\lambda} \quad . \tag{26}$$

In eq. (26) $p_i(\lambda)$ is the i^{th} component of the momentum of particle λ. The sum is over all observed particles. The quantities F_{ij} define a second-rank tensor which can be diagonalized by performing a

rotation to the principal axes. The angle of rotation is just the angle between the directions of maximum energy flow and the beam. A difficulty with direct comparison between theory and experiment is that there is a considerable fluctuation[31] in the number of observed fragments which gives rise to distortions in the kinetic energy flow analysis. However, there are ways around this difficulty; the resulting calculations[32] show good agreement with 400 MeV per nucleon Nb on $_{Nb}$ data[33].

It will be interesting to compare the results of the calculations with data from either heavier mass systems or for higher bombarding energies. As will be discussed in the next section, at higher energies transparency will become important. The effects should be manifested through a small flow angle then calculated with a one-fluid model.

A difficulty with the expression for Eqn. 26 is that it is the non-relativistic kinetic energy tensor. Although one can still construct the tensor for highly relativistic particles, it will no longer have the significance of energy flow. An alternate method[29] to describe flow is thrust. It has been used previously in e^+e^- annihilations and has the desirable property that it uses only relativistically defined quantities. The directed thrust is

$$\mathcal{T}(\hat{n}) = \frac{\sum_i |\vec{p}_i \cdot \hat{n}|}{\sum_i |\vec{p}_i|}$$

where $\hat{n}$ is a unit vector and the sum is over all particles. $\mathcal{T}$ solidifies the inequality $0 \leq \mathcal{T}(\hat{n}) \leq 1$. The thrust is the maximum value of the directed thrust when $\hat{n}$ is varied over all directions.

Thrust has not been used to analyze data from heavy ion experiments. However, it should be very useful to examine momentum flow and transparency for both low and high bombarding energies.

4. THE TWO-FLUID MODEL

As discussed in the previous section, the assumption in hydrodynamics of a very short mean free path is quite reasonable at 200 MeV per nucleon. However, at 1 GeV σ_{NN} is 40 mb, λ_{coll} is around 1.7 fm and λ_{stop} is around 7 fm. This is less than the diameter of a Uranium nucleus but comparable to the diameter of Ca. Thus, the one fluid model discussed in section 3 becomes less relevant at high energies because the nuclei become partially transparent.

To overcome this problem a two-fluid model was introduced[34]: each nucleus is assumed to be a fluid which has the identical properties of the fluid representing the other nucleus. When the two fluids collide they are allowed to exchange energy and momentum at a rate proportional to the relative velocity of the two fluids and to the NN cross section for that velocity. Thus, the rate of momentum loss of each nucleus is finite and the fluids may interpenetrate. The amount of interpenetration is small at low energies where σ_{NN} is large, but may become appreciable when the incident energies are large.

To obtain the equations which describe the motion of the two fluids, recall that the Euler equations ensure the conservation of particle number, energy and momentum. Each of the quantities N_i, E_i and $\vec{P}_i$ will now have a subscript 1 or 2 depending on whether the quantity described is fluid 1 or fluid 2. The equations ensuring particle number conservation will remain unchanged, but those ensuring energy and momentum conservation must be modified to allow an interchange of these quantities. The changes will be in the form of additional terms on the right-hand side of eqs. (11) and (13) which will regulate the rate of change in E_i and $\vec{P}_i$. A derivation may be found in ref. 35.

The resulting generalized Euler equations for fluid one are

$$\frac{\partial \vec{P}_1}{\partial t} + \nabla\cdot(\vec{v}_1\cdot\vec{P}_1) = -\nabla P_1 - R_{coll}\,\frac{K}{Y}\,(\gamma_1\vec{v}_1 - \gamma_2\vec{v}_2) \quad .$$

$$\frac{\partial E_1}{\partial t} + \nabla(\vec{v}_1 E_1) = -\nabla(\vec{v}_1 P_1) - R_{coll}\,\frac{K}{Y}\,(\gamma_1 - \gamma_2) \quad . \tag{27}$$

The quantity Y is $(u_1\cdot u_2)$, $R_{coll} = n_1 n_2 \sigma v_{rel}$ and K is an energy dependent coupling function. Its form is taken from experiment. At low energies K is 0.25 while at higher energies K must approach the value of 1.5 in order to reproduce the stopping power extracted by Busza and Goldhaber[36] from 200 GeV proton scattering on nuclei[37]. Expressions for K may be found in ref. 34 and 38. The expression for fluid 2 is found by interchanging the indices 1 and 2.

Unlike the one-fluid model, the equations for the two-fluid model are not scale invariant. Hence, there will be a dependence on the mass

of the colliding nuclei, but as noted above, this is entirely reasonable and desirable.

The form of the additional terms in eq. (27) is not too surprising, although they have interesting implications which may be seen by examining various limits. If the two nuclei are moving with identical velocities, the two additional terms are zero. However, if $\vec{v}_1 = -\vec{v}_2$ as would be the case in the center-of-mass, the additional term in the energy equation is zero, but not for the momentum equation. Thus, the fluids will slow down because they exchange momentum, but they are not exchanging energy. The internal energy of each fluid must rise. One might think of this as the nucleons moving off their mass-shell. It is also clear from the form of eq. (27) that the additional terms conserve total energy and momentum.

In fig. 5 are shown results of calculations of ^{238}U on ^{238}U at 800 MeV and 31.325 GeV; the equivalent center-of-mass energies are 182 MeV per nucleon and 3 GeV per nucleon. One may compare the former results

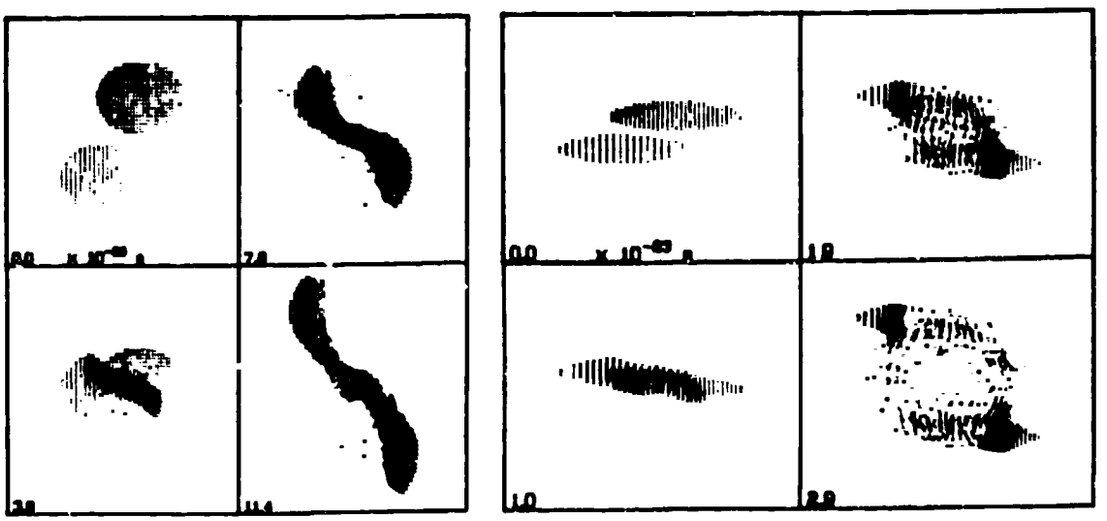

Fig. 5. The time evolution of the density distribution calculated for ^{238}U or ^{238}U at 182 MeV (left-side) and 3 GeV (right-side) per nucleon in the center-of-mass using the two-fluid model. The numbers in the lower-right hand corner of each frame is the time in units of 10^{-23} seconds, (in the center-of-mass). Since the two-fluid model is not scale-invarient, the reaction time is defined.

with those for the one-fluid code in fig. 3. The effect of introducing Although much of the nuclear matter has passed through the other nucleus, the results of the drag are evident. Indeed, a small amount of each nucleus is left inside the other nucleus.

The conditions appropriate for creating a quark-gluon plasma are high density and temperature. In some scenarics it is preferred that the central region be devoid of baryons; in other scenarios this is not necessary. Using two-fluid hydrodynamics one can investigate the initial conditions necessary to produce a given set of criteria. E.g., one might wish to know the minimum bombarding energy necessary for the nuclei to pass through each other, and what the maximum density is and for how long is the density maintained.

The calculations shown in fig. 5 were in three dimensions. As the bombarding energy increases, the Lorentz contraction increases and greater resolution is required. This increases the amount of computer storage and time required. Consequently, at the highest energies the calculations were performed in one dimension.

In fig. 6 are shown the density profiles achieved in the reaction ^{238}U on ^{238}U at 5 GeV on 5 GeV and in fig. 7 for 15 GeV on 15 GeV. One may see from the figures that quite large rest frame densities are

Figs. 6 and 7. The density profiles as a function of time predicted by a one-dimension two-fluid model for ^{238}U on ^{238}U at 5 GeV on 5 GeV (fig. 6) and 15 GeV on 15 GeV (fig. 7). Lower left-hand corner is time in units of 10^{-23} s.

achieved although these densities persist for only a very short time.

It must be emphasized that these densities are those which occur in the baryonic region of phase space. There can also be a high hadronic density (mainly pions) in the central or mid-rapidity region. E.g., assuming one works in the center-of-mass frame, then the mid-rapidity region is that which matter is stationary or nearly so. When the nuclei pass through each other, pions and other mesons will be created; they will be essentially at rest in the center-of-mass frame. If their density is sufficiently high, they may form a plasma having net baryon number zero.

5. ANTIPROTON ANNIHILATION

We have seen that in collisions of relativistic heavy ions a volume of highly compressed nuclear matter with a very high temperature is produced. Such conditions may be suuitable for the production of a quark-gluon plasma. We shall see in the next section which summarizes proposals for detecting the presence of such a plasma that one must vary the temperature and density of the compressed matter; this would be done by, e.g., varying the beam energy. An abrupt change in the variety or number of outgoing particles would suggest the occurrence of a phase transition.

One of the original goals of relativistic heavy ions was to investigate the nucleon equation of state. This is an extremely interesting and important problem independent of whether a plasma is ever observed. One way to explore the nuclear equation of state is to vary the energy and mass of the projectiles. A second method is to annihilate anti-matter inside a nucleus and observe the resultant particles. This program has already begun at LEAR. Calculations using the same models as employed for heavy ion reactions have also been done for antiproton annihilation. In this section we summarize the initial results.

Although the fluid dynamic model has theoretical limitations, it has the advantages that it involves the equation of state directly and also allows one to investigate the possible existence of shock waves, the amount of entropy produced and the time evolution of nuclear matter. In section two the criteria for applicability of fluid dynamics to heavy ion reactions was discussed. Each of the criteria are equally well met in $\bar{p}$ annihilation; in fact, for annihilation of slow $\bar{p}$'s, the evolution of the resulting waves moving through the nucleus takes longer than in heavy ion reactions with the result that fluid dynamics may be more applicable.

The calculations employed a mesh of fixed cubical Eulerian cells, twenty of which spanned the nuclear diameter. Since viscosity is ignored, there is no fundamental scale in the problem and the results are equally applicable to all nuclei; for a Pb nucleus each cube would be 0.7 fm a side. The nuclear fluid in the semi-sphere above the symmetry plane was represented by 56,552 Lagrangian marker particles of $3^3 = 27$ marker particles per cell.

For small $\bar{p}$ momenta the $\bar{p}$ mean free path estimated using $\lambda = 1/\sigma\rho$ is on the order of 0.5 fm. Estimates obtained with an optical-limit, extended Glauber model which takes into account the attractive $\bar{p}$-nucleus optical potential suggest the $\bar{p}$ may penetrate significantly further into a nucleus than the above estimate. Although the vast majority of annihilations will thus occur in the most superficial regions, a few percent will penetrate three mean free paths. The annihilation in the current calculations was assumed to take place at rest 1.4 fm or two cells from the surface. It was assumed that the primary decay mode is to pions, that the pions have a very short range in nuclear matter since most of them will have kinetic energy in the region of the πN resonance, and consequently are all immediately absorbed. Independent of the annihilation products, it was assumed the entire annihilation energy of 1.87 GeV appears as thermal energy uniformly distributed throughout a cube of 8 cells of 1.4 fm a side.

Analyses of pion correlations produced from hadron-hadron collisions suggest a radius of the pion production region[49,41] near one fm. As one or more pions may be expected to traverse the distance to the near surface and thereby excape absorption, the present assumption produces the maximum trauma to the nucleus.

The time evoluation of the density one fm either side of the central plane is shown in fig. 8. The calculation assumed the equation of state shown in fig. 1 having K = 200 MeV. The marker particles are initially aligned in planes so that in the direction perpendicular to the page, each column of marker particles appears as a single point. This alignment is disturbed as the matter evolves giving a graphic representation of any waves which may propagate.

Initially a fireball is formed which forces nuclear matter away from the annihilation region. The matter nearest the surface is flung outward in a flare; the matter forced into the interior gives rise to a compression wave visible in fig. 8. This compression wave is not a shock wave but propagates through the nucleus with velocity equal to the velocity of sound expected for the compressibility. Immediately behind the sound wave a region of rarefaction is present. After the passage of the wave, the cells have a small, non-zero velocity density; as there is no binding energy or surface tension in the calculation, this residual excitation ultimately results in the nucleus dispersing.

The maximum density attained in the sound wave for the K = 200 case was 1.8 ρ_0; this density was obtained after 2 x 20^{-23} s and remained roughly constant until the wave reached the opposite surface. For K = 800 and 80 the maximum compression was 2.1 and 1.6, respectively. The amount of entropy produced is only 0.06 per nucleon compared to values of 3 6 per nucleon in relativistic heavy ion collisions in which shock waves develop[42]; the entropy is produced only in the first 10^{-23} s.

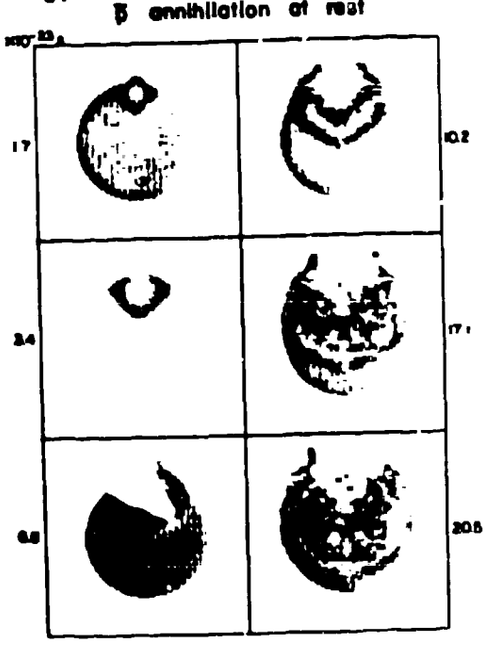

Fig. 8. The time evolution of the central two fm of nuclear matter after the annihilation of an antiproton as calculated in a fluid dynamics model. The nuclear compressibility was 200 MeV. A sound wave may be seen propagating through the nucleus.

After the passage of the sound wave, very little excess thermal energy remained. The amount of kinetic energy the marker particles retained is also small and is on the order of that due to Fermi motion. The nucleus was left in a highly asymmetric shape.

That, save for the first 0.5×10^{-23} s, the annihilation of a $\bar{p}$ results in a region of high density, $\rho \sim 2\rho_0$, but very low temperature is of particular interest as it allows the investigation of the energy per nucleon, e.g., for $\rho > \rho_0$. Although the possibility of a second minimum in $E(\rho)$ for $\rho < 2\rho_0$ seems unlikely[43], $\bar{p}$ annihilation may provide a unique experimental probe for such an investigation. It is complementary to heavy-ion collisions which result in regions of high T which tend to wash out effects of changes in $E(\rho)$.

Considerable experimental work has been done using slow $\bar{p}$'s at LEAR[44] and more energetic antiprotons[45]. After the theoretical work described above was completed, it was realized that there were considerable advantages to using energetic antiprotons rather than stopped antiprotons. First, since the annihilation cross section drops with increasing energy, the $\bar{p}$'s penetrate more deeply into the interior of the nucleus. This means the pions which would otherwise immediately escape if produced at the nuclear surface are more likely to be absorbed. Second, the pions resulting from annihilation of an energetic $\bar{p}$ will be forward peaked. The resulting region of high energy density disperses more slowly. Third, the kinetic energy of a $\bar{p}$, if converted to thermal energy, provides a means of varying the amount of energy deposited.

For energetic pions one must take into account the hadronization length. The fact that some pions have a long mean free path in addition to the hadronization length ensures that energy will be deposited near the center of the nucleus, at least up to some $\bar{p}$ incident energy. Above this energy the hadronization length will approach the nuclear diameter and the energy deposition will decrease.

The average energy deposition was obtained from a Monte Carlo calculation. The $\bar{p}$ was assumed to annihilate into pions, the number of which was taken from experiment[46]. The angular distribution of the pions was assumed to be isotropic in the $\bar{p}p$ rest frame. After a hadronization time of one fm/c in the rest frame of the primordial pion, the pion is assumed to deposit half of its remaining energy after each mean free path. The mean free path was calculated from experimental πN cross sections[47]. Thus the slowest pions materialize first; the fastest pions appear last and furthest from the point of annihilation. At the higher $\bar{p}$ energies a significant fraction of the pions failed to come to rest inside the nucleus. This scenario is similar to that of the inside-outside cascade[48]. The zero temperature equation of state used was a quadratic in the square root of the density[20] with compressibility of $K = 200$. The expression for the thermal pressure was that of a non-relativistic Fermi gas.

The resulting temperatures from annihilation of an antiproton with 6 GeV kinetic energy are shown in fig. 9. The maximum compres-

sions attained are very similar to those for stopped $\bar{p}$'s, i.e. ρ_0. However, the temperatures and entropy are much higher. A shock wave now developes. It is apparent that by varying the kinetic energy of the incident $\bar{p}$, one could vary the temperature reached. In particular the equation of state could be investigated for densities $\rho < 2\ \rho_0$; this is not easily done using heavy ions since the densities there are much higher.

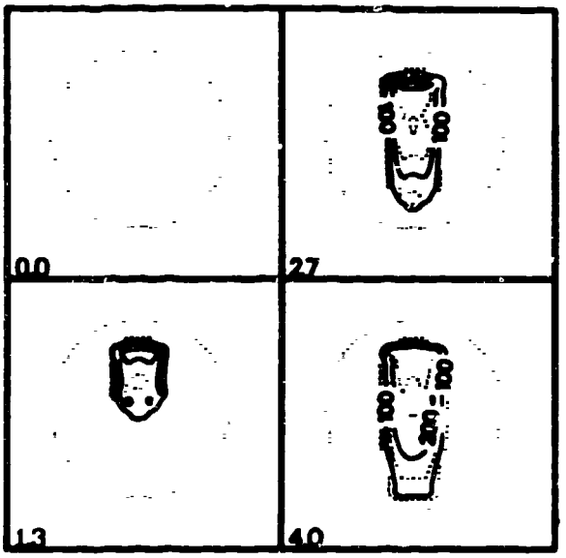

Fig. 9. Temperature contours from the annihilation of a 6 GeV $\bar{p}$. The zero temperature equation of state is that shown in figure 1 with K = 200 MeV. The time in the lower left-hand corner is in units of 10^{-23} s.

Calculations have also been done by W. R. Gibbs[44,49] using an intranuclear cascade code. As already noted the assumptions implicit in a cascade approach are diametrically opposite those of hydrodynamics. It is therefore of interest and also reassuring that the results from his intranuclear cascade code are very similar to those of hydrodynamics. The cascade code predicts maximum densities of 1.5 ρ_0 and initial temperature of around 180 MeV for 6 GeV/c antiprotons. They also suggest the usefulness of antideuteron annihilation if such beams become available.

The initial results presented here must yet be verified by experiment. The initial conditions assumed in the calculations may need to be modified as data becomes available. However, the calculations suggest that $\bar{p}$ annihilation will be a very fruitful and exciting area in the future.

6. SIGNALS FROM COMPRESSED HADRONIC MATTER

In the previous section we have discussed exploring the nuclear equations of state and formation of a quark-gluon plasma. It is apparent that since one detects particles emerging from the reaction volume only long after the plasma or the compressed nuclear matter has expanded, considerable ingenuity is required to devise 'thermometers' with which one can measure the temperatures of the fireball or the amount of compression attained. In this section we discuss some results from recent heavy ion experiments which are indicative of the equation of state and suggestions of the signals from a plasma. A more complete discussion may be found in references 1 and 2.

As an example of the problems associated with extracting a temperature or compression from the products of heavy ion reactions, we first discuss π^+ production from Ar on a KCl at 800 MeV per nucleon. Until recently the situation could be summarized by the statement that hydrodynamic calculations produced too few pions[41] and intranuclear cascade calculations (INC)[9] produced too many when compared with experiment[50]. One of the obvious differences between hydrodynamics and the INC is the latter does not explicitly contain compressional energy. If some of the energy in the INC calculation which would otherwise go into pion production could be diverted into compressional energy, then π production would be a very nice method of extracting the equation of state. This has been done by Stock and his collaborators[51] who have extracted an expression for the equation of state.

The work demonstrates a beautiful interplay between theory and experiment. However, there are some problems associated with their derivation of $E(\rho)$. First, it is assumed that the number of pions observed is the same number as exist when the matter is highly compressed, i.e., there is chemical equilibrium during the expansion phase. However, one might naively assume that during expansion the number of pions actually decreases as pions are absorbed. Further, there is an internal inconsistency with the arguments leading from the INC to an expression for $E(\rho)$: the assumed compressional energy must give rise to a pressure which would tend to keep compression down. This is ignored. Finally, recent INC calculations[52] which take into account effects previously ignored predict pion production rates in much better agreement with experiment, without invoking contributions from compression.

The above discussion on pion production at relatively modest energies at which the physics is presumably better known illustrates the difficulties which must be met at the much higher energies. Generally speaking, the proposed signals from a quark-gluon plasma fall into two categories: the first is production rates of particles with a small cross-section which enables them to escape the highly compressed region of matter. The second class involves strongly interacting particles which are produced in the plasma and which survive either by virtue of selection rules prohibiting their absorption or because chemical equilibrium ensures their number conservation.

The original suggestion was dileptor pairs[53,54] because of their

small cross section. A difficulty with the dilepton signal is the background from usual Drell-Yan mechanism. Recent calculations[54] indicate that the production in a plasma might be appreciably smaller than the Drell-Yan production. Fortunately, experiments can be done at lower energies to explore the problem.

A second particle which has a long mean free path and would be created in a plasma if the temperature is sufficiently high on the J/Ψ particle through charm production. Calculations[55] suggest that charm production would be suppressed in a plasma over that from a normal or non-plasma environment.

Another proposal for a signal is strangeness production[56,57]. In a plasma the Pauli principle would tend to inhibit further production of u and d quarks but not s quarks. Consequently, one should see an enhancement in strange particle production as one passes through the threshold for plasma production.

A number of other possible signatures have been proposed These relate to the amount of entropy produced[58], the relation between transverse momentum and multiplicity[59] and antiproton production[60]. The sharpness of any signature invariably depends on the order of the transition from normal hadron matter to the plasma. It is apparent that the search for the quark-gluon plasma will be both arduous and exciting.

REFERENCES

1. *Quark Matter Formation and Heavy Ion Collisions*, edited by M. Jacob and J. Tran Thanh Van, Phys. Reports 88, 321 (1982).
2. *Quark Matter '84*, edited by K. Kajantie, Springer-Verlag (Berlin, 1985).
3. J. Rafelski, Phys. Letts. 91B, 281 (1980).
4. D. Strottman and W. R. Gibbs, Phys. Letts. 149B, 288 (1984).
5. J. R. Nix, Prog. Part. Nucl. Phys. 2 (1979) 237.
6. H. Stöcker, J. Hofmann, J. A. Maruhn, and W. Greiner, Prog. Part. Nucl. Phys. 4 (1980) 133.
7. S. Nagamiya and M. Gyulassy, *Advances in Nuclear Physics*.
8. A. S. Goldhaber and H. H. Heckman, Ann. Rev. Nucl. Part. Sci., 28 (1978) 161.
9. J. Cugnon and J. Vandermeulen, to be published. J. Cugnon, Nucl. Phys. A387, 191c (1982).
10. L. D. Landau and E. M. Lifschitz, *Fluid Mechanics*, Perganon Press (Oxford, 1959).
11. G. Buckwald, L. P. Csernai, J. A. Maruhn, W. Greiner and H. Stöcker, Phys. Rev. C24, 135 (1981).
12. D. Strottman, to be published.
13. K. Huang, *Statistical Mechanics*, J. Wiley and Sons (New York, 1963).
14. W. R. Schowalter, *Mechanics of Non-Newtonian Fluids*, Pergamon Press (Oxford 1978).
15. O. Bernary, L. R. Price and G. Alexander, LRL Report No. UCRL-20000 NN, 1970.
16. S. Weinberg, *Gravitation and Cosmology*, J. Wiley (New York, 1972).
17. N. L. Balazs, B. Schürmann, K. Dietrich and L. P. Csernai, Nucl. Phys. A424, 605 (1984).
18. W. D. Myers, Atomic Data Nucl. Data Tables, 17, 411 (1976).
19. J. P. Blaizot, D. Gogny and B. Grammaticos, Nucl. Phys. A265, 315 (1976).
20. J. R. Nix and D. Strottman, Phys. Rev. C23, 2548 (1982).
21. A. A. Amsden, F. H Harlow and J. R. Nix, Phys. Rev. C25, 2059 (1977).
22. V. M. Galitskii and I. N. Mishustin, Sov. J. Nucl. Phys. 29, 181 (1979).
23. F. H. Harlow, Los Alamos Scientific Report, LAMS-1956.
24. F. H. Harlow, A. A. Amsden and J. R. Nix, J. Comp. Phys. 20, 119 (1976).
25. A. Sandoval *et al*, Phys. Rev. C21, 1321 (1980).
26. R. Stock *et al*, Phys. Rev. Lett. 44, 1243 (1980).
27. H. Stöcker *et al*, Phys. Rev. Lett. 47, 1807 (1981).
28. M. Gyulassy, K. A. Fraenkel and H. Stöcker, Phys. Lett. 110B, 185 (1982)
29. J. I. Kapusta and D. Strottman, Phys. Lett. 103B, 269 (1981).
30. J. Cugnon, J. Knoll, C. Riedel and Y. Yariv, Phys. Lett 109B, 167 (1982).
31. P. Danielewicz and M. Gyulassy, Phys. Lett. 129B, 293 (1983).
32. G. Buchwald, G. Graebner, J. Theis, J. Maruhn, W. Greiner and H. Stöcker, Phys. Rev. Lett. 52, 1590 (1984).

33. H. A. Gustafsson *et al*, Phys. Rev. Lett. 52, 18 (1984).
34. A. A. Amsden, A. S. Goldhaber, F. H. Harlow and J. R. Nix, Phys. Rev. C17, 2080 (1978).
35. D. Strottman, in *Collective Phenomena in Atomic Nuclei*, edited by T. Engeland, J. Rekstad, and J. S. Vaagen, World Scientific Press (Singapore, 1984).
36. W. Busza and A. S. Goldhaber, Phys. Lett. 139B, 235 (1984).
37. A. E. Brenner *et al*, Phys. Rev. D26, 1497 (1982).
38. A. S. Goldhaber and D. Strottman, to be published.
39. N. J. DiGiacomo, J. Phys. 67, L169 (1981).
40. M. Deutschmann *et al*, Nucl. Phys. B103, 198 (1976).
41. C. Ezell *et al*, Phys. Rev. Lett. 38, 875 (1977).
42. J. I. Kapusta and D. Strottman, Phys. Rev. C23, 1282 (1982).
43. P. Hecking and W. Weise, Phys. Rev. C20, 1074 (1979).
44. N. DiGiacomo, BAPS 29, 643 (1984).
45. F. O Breivik, T. Jacobsen and S. O. Sørenson, Phys. Scr. 28, 361 (1983).
46. G. D. Patel *et al*, Z. Phys. C12, 189 (1982); P. Johnson *et al*, Nucl. Phys. B173, 77 (1980).
47. G. Höhler *et al*, *Handbook of Pion-Nucleon Scattering*, (Fachinformation Zentrum, Karlsruhe).
48. R. Anishetty, P. Koehler and L. McLerran, Phys. Rev. D22, 2793 (1980).
49. W. R. Gibbs and D. Strottman, *Proc. International Conference on Antinucleon and Nucleon-Nucleus Interactions*, Telluride, to be published.
50. S. Nagamiya *et al*, Phys. Lett. 81B, 147 (1979); M.-C. Lemaire *et al*, Phys. Lett. 85B, 38 (1979).
51. R. Stock *et al*, Phys. Rev. Lett. 49, 1236 (1982); J. W. Harris *et al*, LBL Report 17404 (1984), to be published.
52. Y. Kitazoe *et al*, Phys. Lett. 138B, 341 (1984).
53. G. Domokos and J. I. Goldman, Phys. Rev. D23, 203 (1981).
54. K. Kajantie and H. Miettinen, Zeit. Phys. C9, 341 (1981).
55. J. Cleymans and C. Vanderzande, Phys. Lett. 147B, 186 (1984).
56. J. Rafelski and R. Hagedorn, *Proc. Symp. on Statistical Mechanics of Quarks and Hadrons*, edited by H. Satz, North-Holland Publishing Co. (Amsterdam, 1981)
57. J. Rafelski and B. Müller, Phys. Rev. Lett. 48, 1066 (1982).
58. L. P. Csernai and B. Lukács, Phys. Lett. 132B, 295 (1983).
59. L. van Hove, Z. Phys. C21, 93 (1983).
60. U. Heinz, P. R. Subramanian and W. Greiner, Z. Phys. A318, 247 (1984).